IX International Conference on Computational Bioengineering
ICCB2022
P. R. Fernandes and J. Folgado (Editors)

A MULTISCALE FINITE ELEMENT MODEL OF THE ELECTRICAL PROPERTIES OF THYROID TISSUE

Malwina Matella[*+], Dawn C. Walker[*+], Keith Hunter[†+]

[*]Department of Computer Science, University of Sheffield
S1 4DP, Sheffield, UK
mmatella1@sheffield.ac.uk
d.c.walker@sheffield.ac.uk

[†]School of Clinical Dentistry, University of Sheffield
S1 3JD, Sheffield, UK
k.hunter@sheffield.ac.uk

[+]Insigneo Institute for In Silico Medicine
S1 3JD, Sheffield, UK

Keywords: Electrical Impedance Spectroscopy, Finite Element Modelling, Thyroid Tissue Structure, Tissue Type Discrimination

Abstract: Electrical Impedance Spectroscopy (EIS) can be used to measure the electrical properties of biological tissues and has the potential of enhancing tissue differentiation during thyroidectomy. In this study, a finite element-based multiscale model is proposed in order to gain a better understanding of the effect of the follicular structure on the electrical properties of thyroid tissue. To overcome the computational resources limitations, a multiscale modelling approach is implemented. Several input parameters, comprising geometrical variability, different organisation of follicles and material property uncertainties, have been investigated. The results show that the variation in follicle sizes affects mainly the impedance magnitude for frequencies below 10kHz, but the organisation of these structures in thyroid tissue has a little effect on the resultant impedance, if the volumetric ratio of the model compartments is kept constant. In the future, our proposed modelling pipeline will be adjusted to the requirements of parathyroid tissue which exhibits more compact cellular structure compared to the thyroid gland. The ultimate aim is to identify differences in the theoretical EIS spectra, in order to support the clinicians in the EIS guided thyroidectomy procedure.

1 INTRODUCTION

Thyroidectomy is a surgical procedure that relates to total or partial excision of thyroid gland due to various benign or malignant pathologies. Despite its well-established protocol, the procedure can be associated with several post-surgical complications, such as hypoparathyroidism or hypocalcaemia, both resulting from unintended damage of parathyroid glands which are located on the posterior wall of the thyroid. Currently, surgeons rely on their own experience to locate and preserve the parathyroid glands, however, introducing an imaging tool to guide the clinicians during the procedure has the potential to decrease the risks of the

complications associated with the surgery. To date, fluorescence has been considered as a gold standard to successfully differentiate parathyroid glands from adjacent tissues [1]. Recently, a measurement probe exploiting Electrical Impedance Spectroscopy (EIS) technique emerged as a potential tool for this application. The diagnostic value of EIS has already been demonstrated in numerous studies that indicate that the technique can enhance tissue differentiation or the assessment of tissue pathologies [2], [3]. The device (Figure 1) measures the electrical impedance of the tissues after exposing them to the alternating current of known magnitude over a range of frequencies. In the cases of biological tissues, the real part of impedance is expected to fall with the increase of frequency, due to the polarisation of cell membrane occurring in the kHz-MHz region, called β dispersion [4].

Figure 1 Electrical Impedance Spectroscopy device: (a) ZedScan™ [5], (b) tip of the tetrapolar probe showing the principle of the measurement, a known current I flows between the active electrodes (I_1 and V_0) while the passive electrodes (V_1 and V_2) capture the potential difference at different frequencies

The low- and high-frequency magnitude of the impedance and the shape of the dispersion depend on several factors, such as geometrical parameters and electrical properties of the structures within each tissue type. Considering the macroscopic differences such as thyroid follicular organisation compared to parathyroid tissue's tight cellular structure, it is anticipated that the EIS probe could enhance the identification and preservation of parathyroid glands.
In order to gain a better understanding of the effect of the follicular structure's morphological features on the measured frequency-dependent electrical properties of thyroid tissue, a finite element-based multiscale model is proposed with the main aim to extend the modelling framework to the parathyroid tissue and to suggest potential improvements to the thyroidectomy surgical technique.

2 METHODS

MODELLING

Finite Element Analysis (FEA) is a well-established numerical method in the area of solving electric field problems, including those applied to biological systems. Due to the complexity of the biological structures, FEA seems to be a more appropriate tool for our study than analytical methods, such as Maxwell's Mixture Theory [6], that requires high level of geometry and biology simplification that could not be applied to thyroid tissue.

A quasistatic electric analysis is an approach that allows the simulation of an alternating electrical field without the need of running computationally demanding transient simulations. The electromagnetic field is viewed as quasistatic for this type of analysis, since the time-harmonic electrical and magnetic fields remain uncoupled [7]. For the quasistatic electric analysis, the software is solving following governing and continuity equations (Eq. 1 and 2):

$$\{E\} = -\nabla V \tag{1}$$

$$\nabla \cdot \left(\{J\} + \left\{ \frac{\partial \{D\}}{\partial t} \right\} \right) = 0 \tag{2}$$

where $\{E\}$ is electric field intensity vector, V – electric scalar potential, $\{J\}$ – current density vector, and $\{D\}$ – electric flux density vector. The differential equation for electric scalar potential for the time-harmonic analysis takes the form of Eq. 3:

$$-\nabla \cdot ([\varepsilon]\nabla V) + \frac{i}{\omega} \nabla \cdot ([\sigma]\nabla V) = 0 \tag{3}$$

where $[\sigma]$ relates to electrical conductivity matrix and $[\varepsilon]$ – permittivity matrix, i is the imaginary number and ω is the angular frequency ($\omega = 2\pi f$). The preferred element type for this simulation was SOLID231 – a 3D 20-node current-based electric hexahedral element.

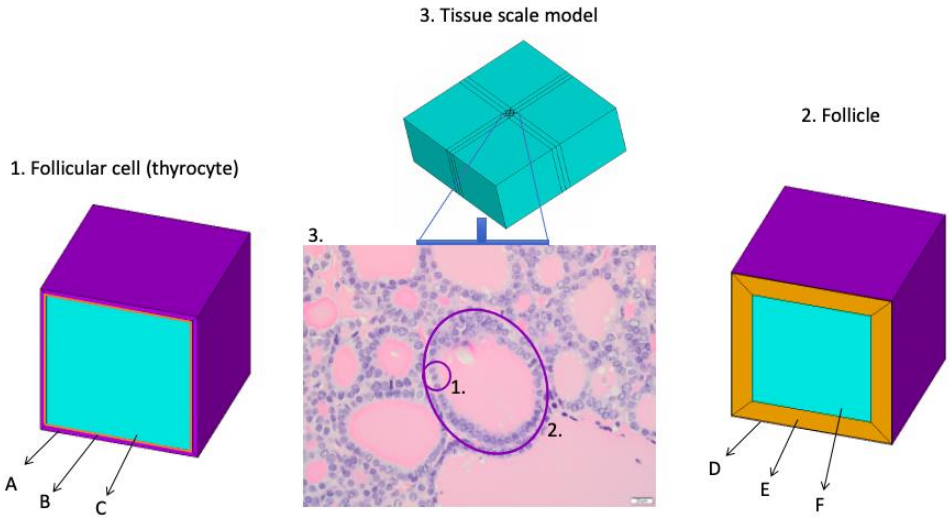

Figure 2 Levels of thyroid multiscale model: a) in the thyroid tissue study: A – extracellular space (ECS), B – cell membrane, C – cytoplasm, D – connective tissue, E – follicular cell compartment, F – colloid

The multiscale modelling approach is incorporated into this study in order to overcome the issues concerning tissue's heterogeneity in the spatial dimension. As mentioned above, the β dispersion measured using an EIS device, results from the capacitive nature cell membrane, which is in order of nm. Including such small structures in a tissue-scale model would not be practical and would require prohibitive computational resources. For this reason, we adopted a multiscale modelling approach, comprising a series of simulations using models representing biological structures from micro- and meso- to macrostructure (Figure 2). Three levels of complexity have been recognised for thyroid tissue: i) follicular cell level, ii) follicle level, iii) tissue scale level. These models are related to each other, as the transfer complex impedance (Z^*) results from micro-scale are assigned to the higher-scale homogenised compartments in a form of material properties, electric conductivity (σ), and relative permittivity (ε_r), calculated from Eq. 4 and 5 at each frequency (f):

$$\sigma(f) = \frac{d}{A * Z'(f)} \tag{4}$$

$$\varepsilon_r(f) = \frac{Y''(f)}{2\pi f * e_0} \frac{d}{A} \tag{5}$$

knowing that:

$$Y''(f) = \frac{-Z''(f)}{(Z'(f))^2 + (Z''(f))^2} \tag{6}$$

where: d and A – thickness and cross-sectional area of the model, e_0 – permittivity of free space, Z' and Z'' – real and imaginary part of impedance, Y'' – imaginary part of admittance. The results from the cell-level model are assigned to the cell layer homogenised compartment in the follicle model, the results of which are in turn assigned to the homogenised tissue scale model.

The tissue scale model recreates the tetrapolar electrodes' arrangement of the EIS ZedScan™ probe (Figure 1a), specifically four electrodes of 0.6 mm in diameter with the centres located on a 2 mm diameter circle, as shown in Figure 3. The resultant impedance is obtained by assigning a known value of current to a drive electrode, while an adjacent electrode is set to ground. The potential difference is calculated from the remaining passive electrodes' voltage values. Impedance at each frequency is calculated as the ratio of resultant potential difference and initial current applied. The dimensions of the tissue scale model are 40x40x15mm. All models have been refined until the numerical results matched with the analytical solution (<1% difference) by comparing the transfer impedance when assigning uniform electrical property to the whole model.

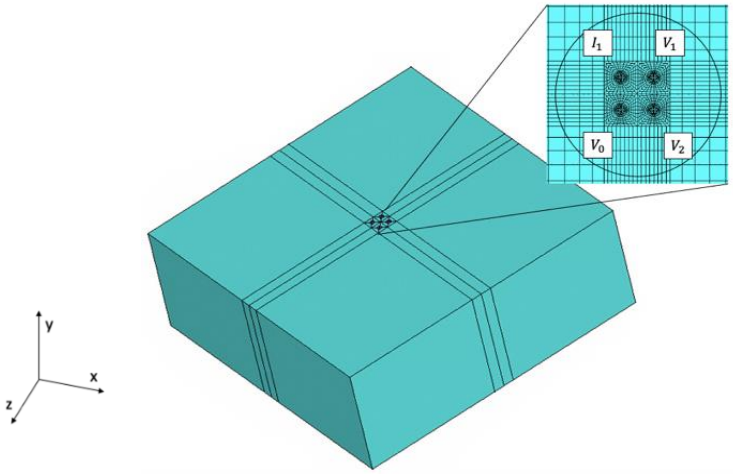

Figure 3 Homogenised tissue scale model with the electrode pattern on the surface recreating the tetrapolar probe arrangement, the electrodes' markers relate correspond to ZedScan™ electrodes arrangement (Figure 1b)

FOLLICULAR MORPHOLOGY

The effect of the natural variability in the sizes of the thyroid follicles on the electrical properties of the whole tissue has been investigated. Since previous computational work in this field [8] evaluated the effects of cellular structure, in this work we focused on the supra-cellular, follicular structure. The modelled follicles sizes have been adjusted according to the values reported in the literature [9] and our own histological measurements (Table 1). The cellular layer properties were generated using cubic cell-scale models assuming a cell length of 8.5 µm, with a cell membrane of 8 nm and ECS thickness set to 0.3 µm. Due to the findings in previous research [8] and more conductive properties of the nuclear membrane in comparison to the cell membrane, the assumption of anucleate cells has been implemented for simplification purposes.

Table 1 Geometrical parameters of follicle model

Geometrical parameters of follicle		
Follicle diameter	d_F [µm]	[50, 100, 150, 200]
Cell layer thickness	d_{cell} [µm]	8.5
Connective tissue thickness	d_{ct} [µm]	[1, 2.5, 5]

The material properties used in the cell model have been set to the averaged values as reported in the literature and summarised in Table 2. Since colloid material has not been studied as broadly as the electrical properties of the cell compartments, properties obtained from similar substances were explored. Thyroid colloid is a semi-solid protein rich material, mainly consisting of thyroglobulin (glycoprotein). Four different materials with significant glycoprotein composition or gel-like characteristics suggested to mimic the electrical behaviour of human soft tissues have been chosen and investigated as potential colloid substitutes. These are: vaginal mucus, egg white, natural gel materials and cytoplasm. The connective tissue properties have been obtained from studies investigating tendon and dura mater, since, similarly to colloid, this material corresponding to thyroid gland has not been studied. The conductivity values are summarised in Table 3. Due to insufficient data, relative permittivity range was obtained from all the aforementioned materials.

Table 2 Material properties used in the thyroid compartments

	Conductivity [Sm^{-1}]	Relative permittivity [-]	Reference
Cell membrane	10^{-7}	8.7	[8], [10]
Cytoplasm	0.55	150.0	[11]–[14]
Extracellular space	1.10	72.0	[11], [14]–[16]
Connective tissue	0.35	10^5	[17]–[19]

Table 3 Material properties of colloid substitutes

	Conductivity [Sm^{-1}]	Reference	Relative permittivity [-]	Reference
Gel materials	0.25	[20]	[50, 70, 87, 150]	[11]–[14] [21]–[23]
Cytoplasm	0.55	[11]–[14]		
Egg white	0.82	[21]–[25]		
Vaginal mucus	1.48	[26]		

EFFECT OF FOLLICULAR ARRANGEMENT

The models presented so far represent simple cubic shapes and very regular arrangements under the assumption that all the repetitive units in the tissue have the same impact on the electrical behaviour of the whole tissue. However, from the biological perspective seen in histology images, the arrangement of structures in the thyroid tissue is much more heterogenous and random, and the effect of different arrangements of follicles in thyroid tissue has been investigated. For this purpose, a single follicle model and two multiple follicles models representing a regular and random arrangement of follicles (Figure 4) have been used to simulate transfer impedance in all directions. All follicles were assigned with mean material properties of a chosen colloid substitute material – cytoplasm – and the models' exterior – with cell properties obtained from the follicular cell simulation. For all models the follicles interior to exterior volumetric ratio was kept constant for three densities of follicles: 10%, 15% and 20%.

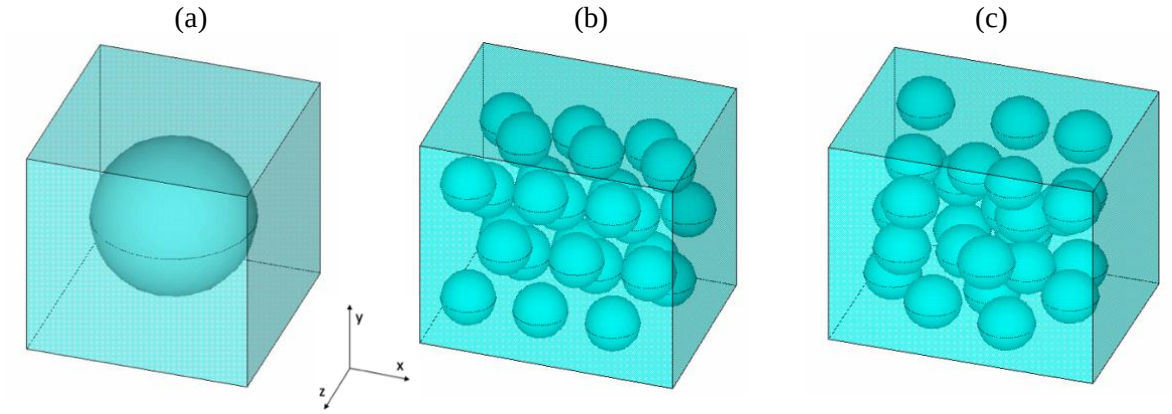

Figure 4 Models for the follicular arrangement study: (a) single spherical follicle model, (b) regular arrangement of hexagonal close packed follicles, (c) random arrangement of follicles

3 RESULTS

All results presented in this section are the real impedance values obtained from the tissue scale model including the material properties obtained from lower-level models at 14 measurement frequencies in the range of 72Hz-625kHz. For the simulations concerning material properties uncertainties, the chosen follicle diameter was 100µm, and 1 µm of connective tissue thickness.

STUDY OF FOLLICULAR MORPHOLOGY

Results showing the impact of two geometrical parameters in the follicle scale are summarised in Figure 5. The effect of follicle size is shown in Figure 5a, which indicates that the real part impedance magnitude before the dispersion decreases when the size of the follicle is increased. Conversely, increased amounts of connective tissue surrounding each follicle decreases the impedance across all simulated frequencies, as depicted in Figure 5b.

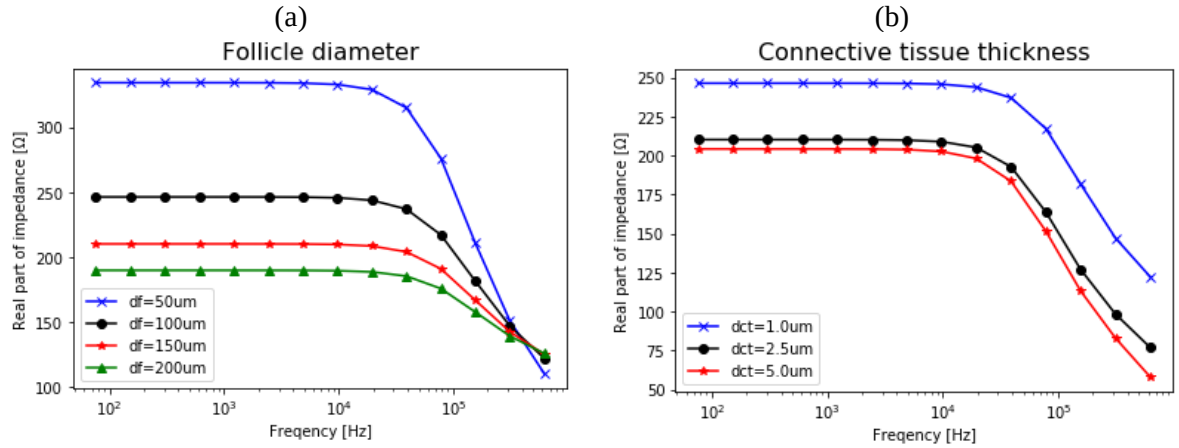

Figure 5 Geometrical parameters variations on the follicle level: (a) diameter of follicle model, (b), connective tissue thickness

Figure 6 shows the effect of the electrical material properties uncertainties associated with the colloid compartment. For the conductivity, four different material substitutes have been investigated and the results shown suggest that the thyroid model is sensitive to the uncertainties in colloid conductivity (Figure 6a) but insensitive to relative permittivity (Figure 6b).

MATERIAL PROPERTY UNCERTAINTIES

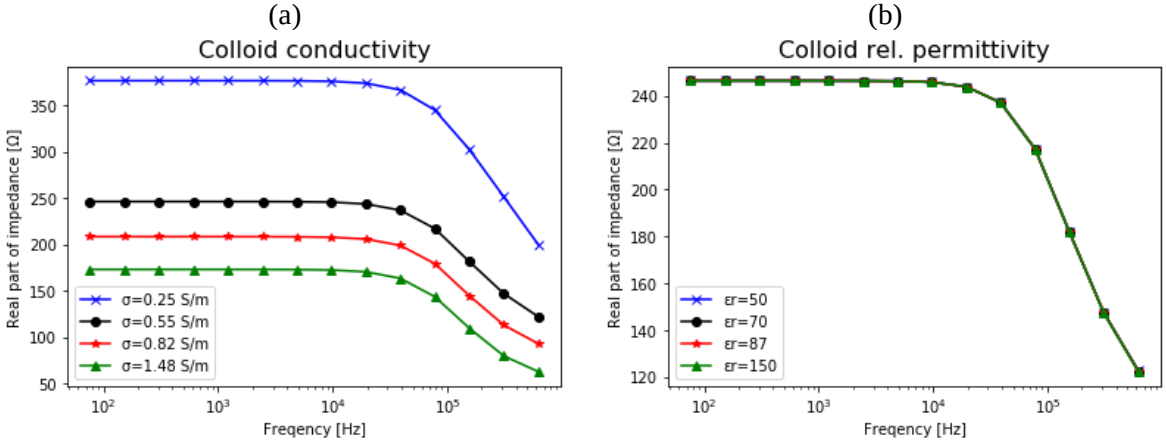

Figure 6 The effects of colloid electrical properties uncertainties: (a) electric conductivity, (b) relative permittivity

EFFECT OF FOLLICULAR ARRANGEMENT

As Figure 7 shows, the results from all models align across all simulated frequencies, suggesting that the specific arrangement of follicles within the tissue is not significant, provided that the volume fraction is maintained.

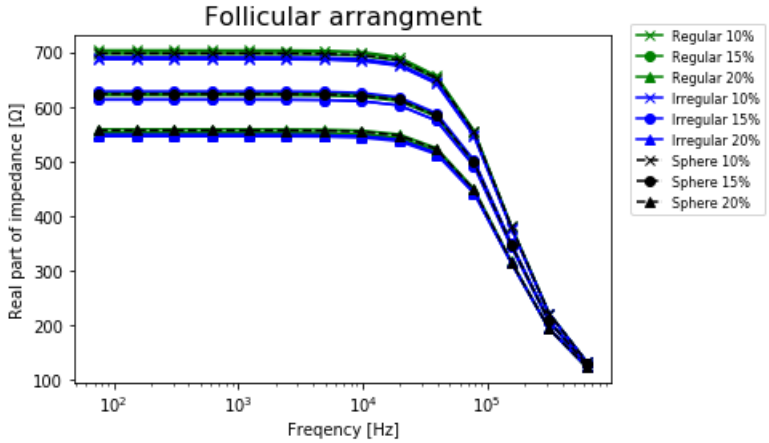

Figure 7 Impedance spectra obtained from three models of different follicle arrangement and complexity

4 DISCUSSION

The proposed multiscale model was constructed to simulate theoretical impedance spectra in order to investigate the electrical behaviour of thyroid tissue in the context of an EIS device-aided thyroidectomy procedure. The impedance spectra simulated when accounting for the uncertainties arising from the natural variation observed in the sizes of structures on the follicle scale, fall within the low- and high- frequency magnitude range of measured spectra documented in the literature (150-700Ω at 72Hz and 70-170Ω at 625kHz) [3]. Given that the results presented in [3] were obtained with the ZedScan™ EIS probe, the geometric properties of which were simulated in our model, this suggests that our multiscale model of thyroid tissue has the ability to reliably predict its electrical behaviour. Additionally, the conductivity range of the material obtained from the follicle scale level and applied to the tissue model fell into the range of 0.2-0.4 Sm^{-1} at 72Hz. Those values are of the same order of magnitude and lie

close to thyroid conductivity of 0.5 Sm^{-1} measured and published in another experimental study [17]. The spectra that do not fit into the experimental range are those representing models with thicker connective tissue layers separating each follicle, which suggests the assumption of 1µm thickness gives more realistic results.

The outcome of the study investigating the size of the follicles (Figure 5a) suggests lower impedance values should be expected for larger follicles. This can be explained by the presence of an increased volume fraction of relatively conductive colloid material for larger follicles.

The simulations concerning the potential colloid material substitutes indicates that this compartment has a significant impact on the results which fall in the range of 150-200 Ω for each frequency point. The material properties of cytoplasm and egg white give the closest results when comparing them against the measured data [3]. Figure 6b shows our model is insensitive to the uncertainty in the relative permittivity of colloid.

Finally, the follicle arrangement study suggests that for the thyroid tissue case, the arrangement of those structures plays a minor role on the electrical behaviour of the macrostructure as long as the volumetric ratio of the studied compartments remains constant. This validates the applicability of using a simplified regular arrangement of follicles with boundary conditions applied to exploit assumptions of symmetry in future modelling work.

In summary, our study suggests that the main factors that impact on the electrical properties at the mesolevel is the volumetric ratio and the material properties of the compartments. However, it is worth noting that only a small range of follicle densities have been studied due to the limitations in creating a more complex model with random distribution of follicles. Moreover, further quantitative comparison between theoretical and experimental results is required. Further computational work will extend the presented modelling pipeline to recreate and simulate the behaviour of the parathyroid tissue with the main aim to understand the differences in the electric impedance spectra which could allow differentiation between these tissue types during surgical procedures.

5 CONCLUSIONS

We have presented a multiscale approach to simulate the electrical properties of thyroid tissue depending on lower level tissue structures, and in particular, the characteristics of follicles. Our results agree well with those previously reported as EIS measurement from human thyroid tissue, but suggest that the size of the follicles, and the unknown properties of the internal colloid may be important in determining the measured impedance values, whereas the exact arrangement of the follicles for a given volume fraction is not important. Future work will extend our methodology to model parathyroid with the aim of informing the use of EIS for tissue discrimination during thyroidectomy.

Acknowledgments: The authors wish to thank Zilico Limited for partially funding the study.

REFERENCES

[1] S. W. Kim, H. S. Lee, and K. D. Lee, “Intraoperative real-time localization of parathyroid gland with near infrared fluorescence imaging,” *Gland Surg.*, vol. 6, no. 5, pp. 516–524, Oct. 2017.

[2] D. C. Walker, B. H. Brown, A. D. Blackett, J. Tidy, and R. H. Smallwood, “A study of the morphological parameters of cervical squamous epithelium,” *Physiol. Meas.*, vol.

24, no. 1, pp. 121–135, Jan. 2003.
[3] S. L. Hillary, B. H. Brown, N. J. Brown, and S. P. Balasubramanian, “Use of Electrical Impedance Spectroscopy for Intraoperative Tissue Differentiation During Thyroid and Parathyroid Surgery,” *World J. Surg.*, 2019.
[4] D. Miklavcic, N. Pavselj, and F. Hart, “Electric Properties of Tissues,” in *Wiley Encyclopedia of Biomedical Engineering*, vol. 6, 2006.
[5] Zilico Limited, *ZedScan™ a new standard in colposcopy - technical brochure*.
[6] N. Nasir and M. Al Ahmad, “Cells Electrical Characterization: Dielectric Properties, Mixture, and Modeling Theories,” *J. Eng.*, vol. 2020, p. 9475490, 2020.
[7] ANSYS, “Theory Reference for the Mechanical APDL and Mechanical Aplications,” 2009.
[8] D. C. Walker, “Modeling the Electrical Properties of Cervical Epithelium,” University of Sheffield, 2001.
[9] A. Faggiano *et al.*, “Age-dependent variation of follicular size and expression of iodine transporters in human thyroid tissue,” *J. Nucl. Med.*, vol. 45, pp. 232–237, Feb. 2004.
[10] F. Bordi, C. Cametti, A. Rosi, and A. Calcabrini, “Frequency domain electrical conductivity measurements of the passive electrical properties of human lymphocytes,” *BBA - Biomembr.*, 1993.
[11] T. Kotnik and D. Miklavcic, “Second-order model of membrane electric field induced by alternating external electric fields,” *IEEE Trans. Biomed. Eng.*, vol. 47, no. 8, pp. 1074–1081, 2000.
[12] J. Yang, Y. Huang, X. Wang, X.-B. Wang, F. F. Becker, and P. R. C. Gascoyne, “Dielectric Properties of Human Leukocyte Subpopulations Determined by Electrorotation as a Cell Separation Criterion,” *Biophys. J.*, vol. 76, no. 6, pp. 3307–3314, Jun. 1999.
[13] H. Morgan, T. Sun, D. Holmes, S. Gawad, and N. G. Green, “Single cell dielectric spectroscopy,” *J. Phys. D. Appl. Phys.*, vol. 40, no. 1, pp. 61–70, 2006.
[14] J. Gimsa, T. Müller, T. Schnelle, and G. Fuhr, “Dielectric spectroscopy of single human erythrocytes at physiological ionic strength: dispersion of the cytoplasm,” *Biophys. J.*, vol. 71, no. 1, pp. 495–506, 1996.
[15] L. A. Geddes and L. E. Baker, “The specific resistance of biological material—A compendium of data for the biomedical engineer and physiologist,” *Med. Biol. Eng.*, vol. 5, no. 3, pp. 271–293, 1967.
[16] F. A. Duck, “Chapter 6 - Electrical Properties of Tissue,” in *Physical Properties of Tissues*, F. A. Duck, Ed. London: Academic Press, 1990, pp. 167–223.
[17] C. Gabriel, *Compilation of the dielectric properties of body tissues at RF and microwave frequencies*. King’s College London, 1996.
[18] S. J. Nagel *et al.*, “Spinal dura mater: biophysical characteristics relevant to medical device development,” *J. Med. Eng. Technol.*, vol. 42, no. 2, pp. 128–139, Feb. 2018.
[19] K. Nowak *et al.*, “Optimizing a Rodent Model of Parkinson’s Disease for Exploring the Effects and Mechanisms of Deep Brain Stimulation,” *Parkinsons. Dis.*, vol. 2011, p. 414682, Apr. 2011.
[20] M. A. Kandadai, J. L. Raymond, and G. J. Shaw, “Comparison of electrical conductivities of various brain phantom gels: Developing a ‘brain gel model,’” *Mater. Sci. Eng. C*, vol. 32, no. 8, pp. 2664–2667, 2012.
[21] T. Dinh, M. Wang, S. Serfaty, and P. Joubert, “Contactless Radio Frequency Monitoring of Dielectric Properties of Egg White During Gelation,” *IEEE Trans. Magn.*, vol. 53, no. 4, pp. 1–7, 2017.

[22] J. Wang, J. Tang, Y. Wang, and B. Swanson, “Dielectric properties of egg whites and whole eggs as influenced by thermal treatments,” *LWT - Food Sci. Technol.*, vol. 42, no. 7, pp. 1204–1212, 2009.
[23] C. Bircan and S. A. Barringer, “Use of Dielectric Properties to Detect Egg Protein Denaturation,” *J. Microw. Power Electromagn. Energy*, vol. 37, no. 2, pp. 89–96, Jan. 2002.
[24] H. Darvishi, M.-H. Khoshtaghaza, M. Zarein, and M. Azadbakht, “Ohmic processing of liquid whole egg, white egg and yolk,” *Agric Eng Int CIGR J.*, vol. 14, pp. 224–230, Dec. 2012.
[25] M. Amiali, M. O. Ngadi, V. G. S. Raghavan, and D. H. Nguyen, “Electrical Conductivities of Liquid Egg Products and Fruit Juices Exposed to High Pulsed Electric Fields,” *Int. J. Food Prop.*, vol. 9, no. 3, pp. 533–540, Sep. 2006.
[26] K. Verma *et al.*, “Characterization of physico-chemical properties of cervical mucus in relation to parity and conception rate in Murrah buffaloes,” *Vet. World*, vol. 7, pp. 467–471, Jul. 2014.